Predicting soil moisture conditions across a heterogeneous boreal catchment using terrain indices

Johannes Larson[1], William Lidberg[1], Anneli M. Ågren[1], Hjalmar Laudon[1]

[1]Department of Forest Ecology and Management, Swedish University of Agricultural Sciences, Umeå, 901 83, Sweden

Correspondence to: Johannes Larson (Johannes.larson@slu.se)

Abstract. Soil moisture has important implications for drought and flooding forecasting, forest fire prediction and water supply management. However, mapping soil moisture has remained a scientific challenge due to forest canopy cover and small-scale variations in soil moisture conditions. When accurately scaled, terrain indices constitute a good candidate for modelling the spatial variation of soil moisture conditions in many landscapes. In this study, we evaluated seven different terrain indices at varying digital elevation model (DEM) resolutions and user-defined thresholds as well as two available soil moisture maps, using an extensive field dataset (398 plots) of soil moisture conditions registered in five classes from a survey covering a (68 km2) boreal landscape. We found that the variation in soil moisture conditions could be explained by terrain indices and the best predictors within the studied landscape was Depth to water index (DTW) and a machine learning generated map. Furthermore this study showed a large difference between terrain indices in the effects of changing DEM resolution and user-defined thresholds which severely affected the performance of the predictions. For example the commonly used Topographic wetness index (TWI) performed best on a resolution of 16 m while TWI calculated on higher than 4 m DEM resolutions gave inaccurate results. In contrast the Depth to water (DTW) and Elevation above stream (EAS) were more stable and performed best on 1-2 m DEM resolution. None of the terrain indices performed best on the highest DEM resolution of 0.5 m. In addition this study highlights the challenges caused by heterogeneous soil types within the study area and shows the need of local knowledge when interpreting the modelled results. The results from this study clearly demonstrate that when using terrain indices to represent soil moisture conditions, modelled results need to be validated, as selecting unsuitable DEM resolution or user-defined threshold can give ambiguous and even incorrect results.

1 Introduction

Soil moisture represents plant available water at the land surface that is not derived from groundwater, rivers and lakes, but instead in the pores of the soil. It consists of unsaturated soil, affected by variable temporal and spatial dynamics that regulate fundamental ecosystem functions such as plant growth, nutrient cycling and carbon accumulation (Olsson et al., 2009; Högberg et al., 2017; Wang et al., 2019). Soil moisture also has important implications for drought and flooding forecasting, forest fire

30   prediction and water supply management (Koster et al., 2010; Robock, 2015; O et al., 2020). While temporal variability in soil moisture is largely determined by precipitation, temperature and soil characteristics, topography acts as a first order control of spatial variation in soil moisture within most landscapes (Florinsky, 2016).

Predicting soil moisture patterns across space and time remains an important scientific challenge, limited by large temporal variability, small-scale heterogeneous responses to precipitation inputs and local soil properties. While small-scale

35   spatial variability often limits the use of empirical measurements for upscaling, temporal dynamics superimposed on such heterogeneous patterns create an additional challenge. Due to the effect that topography has on the spatial variation in soil moisture conditions, such information is a fundamental part of soil moisture modelling. A Digital Elevation Model (DEM) is a digital representation of a terrain surface, often generated using remote sensing techniques such as photogrammetry or airborne Light Detection And Ranging (LiDAR). Terrain indices extracted from DEMs have become widely used in soil and

40   hydrologic sciences predicting surface water and groundwater flow paths, and soil moisture conditions.

An early and successful approach to modelling soil moisture conditions was the Topographic Wetness Index (TWI) developed by (Beven and Kirkby, 1979). TWI is a function of both the slope and upslope contributing area, and is still widely used in landscape modelling. TWI has been shown to be sensitive to DEM resolution (Western et al., 1999; Sørensen and Seibert, 2007; Lin et al., 2010) and the specific flow algorithms used (Sørensen et al., 2006; Kopecký et al., 2021). TWI has

45   been followed by several other terrain indices based on similar approaches such as the Downslope index (DI) (Hjerdt et al., 2004), and the Wetness Index based on Landscape position and Topography (WILT) (Meles et al., 2020).

Some topography-based indices use stream networks in the calculations, which are derived from flow accumulation grids such as the Depth to Water index (DTW) (Murphy et al., 2008) and Elevation Above Stream (EAS) (Rennó et al., 2008). Using this approach, streams are defined with a so-called stream initiation threshold, which is the accumulated area required to form

50   surface water. Selecting an appropriate stream initiation threshold has proven to be difficult due to temporal dynamics (Ågren et al., 2015) and soil textures (Ågren et al., 2014). Thresholds, such as stream initiation, used in terrain indices can be as, or even more, important as selecting the correct DEM resolution for the soil moisture modelling.

The use of airborne LiDAR has increased both the accuracy and resolution of DEMs and, as a result, soil moisture modelling (Murphy et al., 2011; Ågren et al., 2014; Leach et al., 2017; Kopecký et al., 2021). However, the resolutions of

55   DEMs used for hydrological modelling must reflect topographic features that are key elements in the hydrological response (Quinn et al., 1995). This means that higher resolutions do not necessarily result in better predictions, as the microtopography does not always control hydrological flow paths. Hence, there is a concern that the development of LiDAR-derived high-resolution DEMs has changed resolutions from being too coarse for small-scale hydrological modelling to being too high for many applications. With the use of terrain indices, there is often an optimal resolution depending on landscape type and specific

60   feature of interest (Gillin et al., 2015). Despite rapid LiDAR development, finding the optimal DEM resolution of terrain indices has remained relatively unexplored, with only a few exceptions (Seibert et al., 2007; Lin et al., 2010; Ågren et al., 2014).

In addition to DEM resolutions and user-defined thresholds, soil moisture modelling using terrain indices must take the local variations in soils and landforms into consideration. Across former glaciated landscapes, soil hydraulic properties are often relatively consistent with unconsolidated ablation till overlaying basal till and/or bedrock. This means that hydrological pathways are significantly affected by the topography, resulting in soil moisture conditions in neighbouring areas differing greatly within short distances because of the local topography (Rodhe, 1987). The topographical effect on hydrological pathways is less pronounced in flat sorted sediment areas due to often low topographic variation and soils with consistent hydrological conductivity at depth (Bachmair and Weiler, 2011). In landscapes with varying quaternary deposits, accurate soil moisture predictions become more challenging (Güntner et al., 2004; Grabs et al., 2009; Zhu and Lin, 2011; Ågren et al., 2014), with consideration of these factors becoming important when interpreting modelled soil moisture.

Recent promising approaches for accounting for landscape and soil variations have combined multiple terrain indices and other mapped information. One example of such an effort is the Swedish Soil Moisture Index (SMI) that combines DTW and the Soil Topographic Wetness index (STI) (Buchanan et al., 2013), and accounts for soil transmissivity estimated from the quaternary deposit maps. An alternative is to use machine learning (Abowarda et al., 2021). Ågren et al. (2021) adjusted the soil moisture maps to local conditions over the whole of Sweden by training the model on field data from 16,000 plots and information from 28 maps. Key to this work were high resolution terrain indices calculated for different resolutions and thresholds. However, while machine learning is an excellent way of generating predictive models, it is difficult to interpret how the model combines indices with multiple resolutions and thresholds for different landscape types. Due to the large applications, wide uses and availability of terrain indices there is a need of understanding the underlying effects of DEM resolution, user-defined thresholds and landscape types have on the modelled results. Using terrain indices to model soil moisture conditions on inappropriate scales and landscape types may result in inaccurate predictions.

The aim of this study was, therefore, to evaluate how DEM resolution, thresholds and landscape types affect soil moisture predictions from a range of readily available terrain indices. We did this by examining which digital terrain index provided the best prediction of field determined soil moisture classes within a heterogeneous but well-studied landscape in the boreal region, the Krycklan Catchment study (Laudon et al., 2020). Using a detailed forest and soil survey that covered the entire catchment allowed a test and performance evaluation of different terrain indices, in order to find the optimal resolutions and thresholds for modelling soil moisture.

2 Methods

2.1 Site description

The 68 km^2 Krycklan Study Catchment is situated in the northern part of Sweden (Lat. 64°, 23′N, Long. 19°, 78′E) (Fig. 1). The catchment has a gentle topography, with a poorly weathered gneissic bedrock and elevations ranging from 127 to 372 m.a.s.l. The highest postglacial relict coastline crosses the area at around 257 m.a.s.l. The upper parts are dominated by glacial till while the lower parts are dominated by sorted sediments of sand and silt. The climate is characterized as a cold temperate

95   humid type with persistent snow cover during the winter season (Laudon et al., 2020). The 30 year mean annual temperature (1986-2015) is 2.1°C, with the highest monthly mean temperature in July and lowest in January (14.6 and -8.6 respectively). The mean annual precipitation equals 619 mm where more than 30% falls as snow. Land cover is dominated by forest (87%) and a mosaic of mires (9%) and lakes. Due to forest management, Krycklan is a complex mosaic of forest stands of different age classes and species composition. Forests are dominated by Scots pine (*Pinus sylvestris* L.) and Norway spruce (*Picea*

100   *Abies* (L.) H. Kartst.) covering 63% and 26% respectively. Understory vegetation is dominated by ericaceous shrubs, consisting mostly of bilberry (*Vaccinium myrtillus*) and cowberry (*Vacinium vitis-ideae*) covering moss mats of *Hylocomium splendens* and *Pleurozium schreberi*. Peatlands and wet areas have a vegetation dominated by *Sphagnum* species (Laudon et al., 2013). Forest soils are dominated by well-developed iron podzol. In addition to analysis over the entire catchment area, Krycklan was divided into two sub areas (till and sorted sediment) according to the quaternary deposits map, in order to analyse the effects

105   of landscape types (Fig. 1).
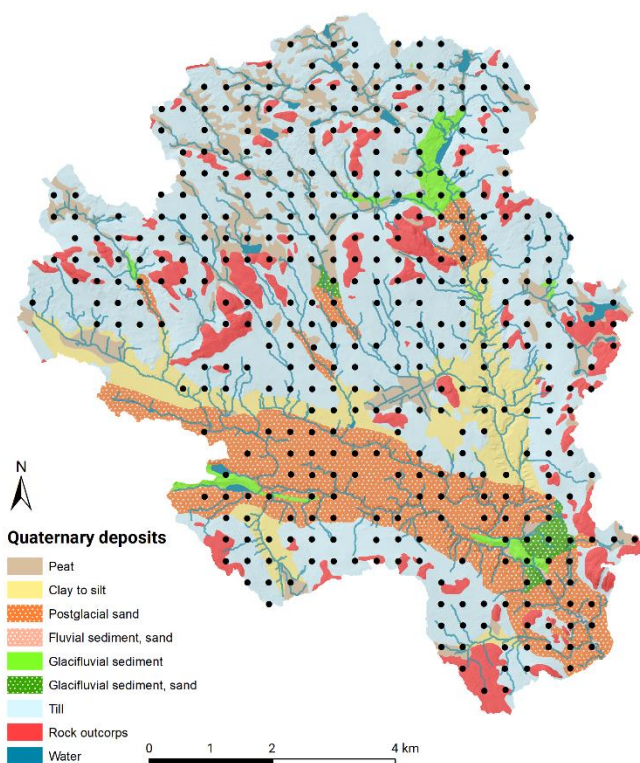
Figure 1: The Krycklan catchment showing the quaternary deposits survey and plots as black circles.

2.2 Forest survey

A forest survey grid was established in 2014, consisting of 500, 10 m radius survey plots (314.15 m^2) covering the entire

110   Krycklan catchment, with each plot spaced 350 m apart. The survey plot locations were calculated using a randomly chosen

origin and oriented along the coordinate axis of the Sweref 99 TM projection. Each nominal plot location was located in the field using a Garmin GPS 62stc GNSS receiver, and plot centres were marked with an aluminium profile. During a revisit, high accuracy centre positions were placed in the field using a Trimble GeoXTR DGPS receiver. Plots without high precision GPS locations, plots located on or outside the catchment boundaries, arable land, lakes and roads were excluded in this study.

115   In total, soil moisture classifications were made for 398 plots during the autumn of 2014 and the spring of 2015.

2.3 Soil moisture field classification

Soil moisture classes were registered in the field following the protocol of the Swedish national forest inventory (NFI) (Fridman et al., 2014), based on an estimation of each plot's average depth to groundwater level during the vegetation period estimated from its position in the landscape, vegetation patterns and soil type. This approach reduces the discrepancies caused

120   by seasonal variation and provides an indicator of the general soil moisture conditions, which is the focus of this study. Survey plots were categorized in five classes dry, mesic, mesic-moist, moist and wet, which are described and presented below and can be found in more detail in the field instruction (Swedish NFI, 2014).

- Dry soils have an average groundwater table more than 2 metres below the soil surface. Dry areas tend coarse- textured

125   and can be found on the top of hills, ridges and eskers. The soils are mainly leptosols, arenosols, regosols or podzols (with thin organic and bleached horizons).

- Mesic soils have an average groundwater table between 1–2 metres below the soil surface. Podzol is the dominating soil type with a thin fairly thin (4-10 cm) organic mor layer covered mainly by dryland mosses (e.g. Pleurozium

130   schreberi, Hylocomium splendens, Dicranum scoparium). They can be walked on dry-footed even directly after rain or shortly after snowmelt.

- Mesic-moist soils have an average groundwater table depth less than 1 metre. Mesic-moist areas are often located on flat ground in lower lying areas, or lower parts of hillslopes. The soils tend to wet up on a seasonal basis. Whether

135   you can cross in shoes and remain with dry feet depends on the season and the time since the last heavy rain or snow melting event. Patches of wetland mosses (e.g. *Sphagnum sp.*, *Polytrichum commune*) are common and trees commonly tend to grow on humps. Podzols are commonly found, but often with a thicker organic layer compared to mesic sites. The organic layer is often classified as peaty mor.

140   - Moist soils have an average groundwater table depth less than 1 metre below the soil surface. The groundwater table is often visible in depressions within the plot. Areas classified as moist are found at lower grounds, at the lowest parts of slopes and flat areas below larger ranges. One can cross in shoes and keep one's feet dry by utilizing tussocks and higher lying areas. When stepping in depressions, water should form around the feet even after dry spells. The

vegetation includes wetland mosses (e.g. *Sphagnum sp.*, *Polytrichum commune*, *Polytrichastrum formosum*). Trees often grow on small mounds and the soil type is most often histosol, regosol or gleysol.

- Wet soils are areas where the ground water table is close to the soil surface and permanent pools of surface water are common. These areas are often located on open peatlands. Drainage conditions are very bad and it is not possible to cross these areas in shoes without ending up with wet feet. Coniferous trees seldom develop into stands. The soil type is most often histosol or gleysol.

2.4 Digital terrain indices

The study utilized a LiDAR-based Digital Elevation Model (DEM) created from an airborne laser scanning in August 2015. A 0.5 x 0.5 m DEM was generated from a point cloud with 10 points per m^2. Horizontal and vertical errors were 0.1 m and 0.3 m, respectively. The DEM was resampled from 0.5 m to resolutions of 1, 2, 4, 8, 16, 32 and 64 m. Nine commonly used digital terrain indices were calculated using DEMs with eight resolutions of 0.5, 1, 2, 4, 8, 16, 32 and 64 m (Table 1). The indices Depth to Water (DTW) and Elevation Above Stream (EAS) use extracted stream networks in their calculations, with the size of the stream network being set by the stream initiation threshold. For each resolution, DTW and EAS were calculated for the stream initiation thresholds 1, 2, 4, 8, 16 and 32 ha, which is the range of the expected variability in the study region. The Downslope Index (DI) was calculated with vertical distances of 2 and 4 m. A total of 146 terrain indices maps of soil moisture were produced. Field plot centre values for all indices maps were extracted for evaluation. All of the digital terrain indices were calculated using Whitebox Tools (Lindsay, 2016b), an open source program developed at the University of Guelph, Canada. The code for aggregating the DEM and the Python code for the calculations can be found in the Supplementary material 1 (S1). In addition to the terrain indices that we calculated from the DEM, we also used two soil moisture maps downloaded from external sources: the SLU soil moisture map (Ågren et al., 2021) and a Soil Moisture Index map (SMI) developed by the Swedish Environmental Protection Agency (Naturvårdsverket, 2021).

Table 1. All indices calculated in this study. Calculations were made for resolutions of 0.5, 1, 2, 4, 8, 16, 32, 64 m.[1]Calculations were also made for stream initiation thresholds of 1, 2, 4, 8, 16, 32 ha.[2] was calculated with vertical distances of 2 and 4 m. All GIS calculations were carried out using Whitebox Tools (Lindsay, 2016b), except for SLU soil moisture map and SMI which were downloaded from other sources.

Digital terrain indices	Abbreviation	Total number of layers
Topographic wetness index	TWI	8
Depth to water	DTW[1]	48
Elevation above stream	EAS[1]	48

Downslope index	DI^2	16
Wetness index based on landscape position and topography	WILT	8
Relative topographic position	RTP	8
Plan curvature	PlanC	8
SLU soil moisture map	SLU	1
SMI	SMI	1

170

2.5 DEM pre-processing and extraction of stream networks

Prior to hydrological modelling, the DEM was pre-processed to make it hydrologically accurate using the two-step breaching approach suggested by Lidberg et al. (2017). This approach works by first carving a short path into the DEM at locations where

175 culverts and previously mapped streams intersect road embankments. Remaining depressions were resolved by a complete breaching approach using the tool Breach depressions in Whitebox Tools (Lindsay, 2016a). Two flow pointer grids and flow accumulation grids (FA) were extracted from the hydrologically corrected DEM using the D-infinity flow routing algorithm (D∞) (Tarboton, 1997) and the multiple flow direction algorithm (MD∞) (Seibert and McGlynn, 2007). D8 (O'Callaghan and Mark, 1984) and D∞ (Tarboton, 1997) are both commonly used and widely implemented flow routing algorithms. MD∞ is an

180 attempt to combine these two approaches and disperses flow like D∞ up to a user-defined threshold (aiming to simulate diffuse groundwater flows), after which it switches to operate like D8 without dispersion (aiming to simulate channelized flow of surface waters). Stream networks were extracted from the flow accumulation raster using stream initiation thresholds 1, 2, 4, 8, 16 and 32 ha. Streams during different conditions can be mapped by varying the stream initiation thresholds. Larger stream initiation thresholds represent streams during low flow conditions while smaller thresholds represent conditions at high flow

185 rates.

2.5.1 Topographic wetness index (TWI)

TWI predicts soil moisture based on local slope and the area's specific catchment area (Eq. 1), where α is the specific catchment area and β is the slope of the grid cells in degrees (Beven and Kirkby, 1979).

$$T_{WI} = \ln(\alpha/tan\beta) \tag{1}$$

190 This was calculated using the D∞ flow algorithm for all eight DEM resolutions.

2.5.2 Depth to Water (DTW)

The Depth to Water index predicts soil moisture using the surface water source grid (stream network) and the surrounding landscape (Murphy et al., 2008). The DTW index refers to the least-cost path from any cell in the landscape to the nearest surface water cell (DTW = 0) channel. DTW is expressed as Eq. (2), where dz_i and dx_i represent the vertical distance between two cells.

$$D_{TW} = \left[\sum \frac{dz_i}{dx_i} a \right] x_c \qquad (2)$$

The constant a is equal to 1 if the path between the cells connects parallel to the cell boundaries or $\sqrt{2}$ if it connects the cell diagonally; x_c is the size of the raster cells. Cells located far away or at higher elevation from the flow channels will have high DTW values, meaning that the cells are drier. Stream cells were calculated using the source layers with extracted streams from the (MD∞) pointer described above. DTW was calculated for each of the six stream initiation thresholds and eight DEM resolutions.

2.5.3 Elevation Above Stream (EAS)

EAS indicates soil moisture by using the source layer with extracted streams described above and the original DEM (Rennó et al., 2008). EAS is calculated from the elevation difference between a grid cell in the landscape and the nearest stream cell calculated from the nearest flow path from the (MD∞) pointer grid. EAS was calculated for each of the six stream initiation thresholds and eight DEM resolutions.

2.5.4 Downslope index

The downslope index represents the length of a flow path required to drop a given vertical distance d (m) (Eq. 3 and Eq. 4) (Hjerdt et al., 2004). The algorithm calculates the distance downslope required to travel in order to descend d metres. Downslope index can be reported both as a distance d and a gradient, $\tan \alpha_d$, where the horizontal distance to the point d metres below follows the steepest directional flow path.

$$tan\ \alpha_d = \frac{d}{L_d} \tag{3}$$

Local linear interpolation is used between the two points to calculate the value of L_d. The slope angle between the starting point and the target point is represented by α_d. For elevation differences approaching zero, the values of $\tan\alpha_d$ approach the local ground surface gradient, $\tan\beta$:

$$\lim_{d \to 0} tan\alpha_d = \tan\beta \tag{4}$$

Downslope index was calculated for 2 m and 4 m as the given vertical distances.

2.5.5 Wetness Index based on Landscape position and Topography (WILT)

WILT assumes that soil moisture is inversely proportional to ΔX and ΔZ in a groundwater-dominated landscape, where ΔZ is the depth to groundwater and ΔX is the horizontal distance to the nearest surface water feature (Eq. 5) (Meles et al., 2020). WILT is a modification of TWI, obtained by dividing the upslope contribution area A by ΔX and ΔZ:

$$WILT = \ln\left(\frac{A}{\Delta X * \Delta Z * \tan\beta}\right) \tag{5}$$

In this study, we calculated WILT where A was the upslope source area using D∞ flow accumulation, as with the TWI calculations. ΔX was derived from the downslope distance to stream and lakes using surface waters. ΔZ was the elevation difference between the DEM and modelled groundwater, represented by a DTW calculated for the property map.

2.5.6 Relative Topographic Position (RTP)

RTP is an index for the local position of a point in the landscape relative to its surroundings, which accounts for elevation distribution (Eq. 6). Within a user-specified local neighbourhood size, the RTP function uses the central elevation relative to the minimum (z_{min}), mean (μ) and maximum elevation (z_{max}):

$$RTP = \frac{(z_0 - \mu)}{(\mu - z_{min})}, if\ z_0 < \mu \ \ or \ \ RTP = \frac{(z_0 - \mu)}{(\mu - z_{max})}, if\ z_0 >= \mu \tag{6}$$

RTP index is bound by the interval of [-1, 1], indicating whether the cell is above or below the filtered mean (Newman et al., 2018).

2.5.7 Plan Curvature (PlanC)

The plan curvature represents the curvature of the surface perpendicular to the direction of the slope direction (Wilson and Gallant, 2000). This index shows the divergence and convergence of slopes, where values are positive for convergent areas and negative for divergent ridges. The plan curvature was chosen for its influence on the downslope convergence and divergence of water flow paths.

2.5.8 Soil Moisture Index (SMI)

We also included an SMI from the national land cover database of the Swedish Environmental Protection Agency (Naturvårdsverket, 2021). This SMI was calculated as (Eq. 7):

$$SMI = \left(0.7 \times \frac{1}{DTW}\right) + (0.3 \times STWI) \tag{7}$$

This is a weighted map combining DTW and a modified TWI calculation, the Soil Topographic Wetness Index (STWI) (Buchanan et al., 2013), which accounts for soil transmissivity estimated from the quaternary deposit maps. The SMI map has a resolution of 10 m.

2.5.9 SLU Soil moisture map

A recent development in soil moisture mapping has been the use of machine learning to combine multiple soil moisture indices into one map (Lidberg et al., 2019; Abowarda et al., 2021; Ågren et al., 2021). Ågren et al. (2021) developed a new soil moisture map of Sweden by utilizing a variety of nationwide information, including the above-mentioned terrain indices, climate data and quaternary deposits. Training data consisted of nearly 16,000 field plots spread across the Swedish forested landscape from the national forest inventory. The final map showed the probability (0–100%) of a soil being wet. The SLU soil moisture map was produced at 2 m resolution, while the input digital terrain indices were calculated in multiple scales.

2.6 Statistics

2.6.1 Orthogonal Projections to Latent Structures (OPLS)

255 To ascertain which digital terrain index provides the best prediction of soil moisture within this heterogeneous landscape, we used Orthogonal Projections to Latent Structures (OPLS) analysis. Field classifications of soil moisture at each plot were used to evaluate the terrain indices through direct plot by plot comparison. OPLS was carried out on the entire catchment. The OPLS was carried out using the multivariate statistical program SIMCA 16.0, Umetrics, Umeå. The method of OPLS is a modification of Partial Least Squares regression (PLS) (Eriksson et al., 2006). In OPLS, the systematic variation in the predictors (X) is

260 divided into two parts: one part that is predictive for the determinant (Y) (in this case, the field-determined soil moisture classes) and the orthogonal i.e. not related to Y. OPLS produces a model with improved interpretability compared to the ordinary PLS method. The method is used to identify important variables for predicting Y and singling out less important variables containing "noise". High positive or negative loadings on the predictive axis (pq[1]) indicate variables that are, respectively, positively or negatively correlated with Y, with increased correlation further away from origin. The orthogonal

265 axis shows how much of the variation for each variable was not correlated with the determinant (Y). Before analysis, all variables were transformed to fit normality using a log transformation in SIMCA. SIMCA 16.0 also calculates the influence of each X variable in the model called Variable Importance on Projection (VIP). VIP components of an OPLS model are VIP predictive, VIP orthogonal as well as VIP total component. The VIP values are regularized such that if all X variables had the same importance for the model, they would all take the value one. VIP values larger than one for either VIP component indicate

270 X variables that are important for that part of the model (Eriksson et al., 2006). Analysis was carried out in SIMCA 16.0 and figures were produced using R version 4.0.2 (R Core Team, 2020) and the package ggplot2 (Wickham, 2016).

2.6.2 Confusion matrix

To evaluate the effects of landscape type i.e. sorted sediment and till soils within the catchment, we used the terrain index that preformed best in the OPLS analyses and its correspondence to the two wettest soil moisture classes (wet and moist). The

275 overall conformance of the best terrain index with the combined wet and moist classes was assessed using confusion matrixes, accuracy (ACC) (Eq. 8) and Matthews Correlation Coefficient (MCC) (Eq. 9). The confusion matrix consists of true positives (TP), so accurately predicted wet plots, and false positives (FP) where dry plots were predicted wet, true negatives (TN), where the map correctly predicted dry plots and false negatives (FN) where the map predicted dry areas on wet plots. Accuracy (ACC) was assessed for each of the plots by:

280 $$Acc = \frac{TP+TN}{TP+TN+FP+FN} \tag{8}$$

The confusion matrix was further evaluated using Matthews Correlation Coefficient (MCC), for which a value of 1 indicates a perfect fit, 0 no better than random predictions and -1 a perfect negative correlation. MCC was calculated as (Eq. 9):

$$MCC = \frac{TP \times TN - FP \times FN}{\sqrt{(TP+FP)(TP+FN)(TN+FP)(TN+FN)}} \qquad (9)$$

285 For unbalanced datasets such as this, MCC is the best measure of model performance (Boughorbel et al., 2017).

3 Results

3.1 Field data

The field survey showed that the dominant soil moisture class was mesic, making up 60% of the survey plots in the catchment (Table 2). Mesic-moist was the second largest class with 15% of the plots; the moist and wet classes each made up 8%. The

290 driest class (dry) made up 10% of the total plots in the catchment. Dividing the catchment into till and sorted sediment areas using the quaternary deposit map (Fig. 1), the proportion of classes became substantially different. Only 6% of the plots in the sorted sediment area were classified as moist or wet, compared to 20% in the till areas. A larger percentage (12%) of plots were found in the driest class in the sorted sediment areas compared to the till areas (9%).

Table 2. Percentage of observations in the five soil moisture classes for the entire Krycklan catchment and divided into till and sorted
295 **sediment areas**

Soil moisture classes

Soil moisture class	Dry	Mesic	Mesic – moist	Moist	Wet	Plots (n)
Entire catchment	10%	60%	15%	8%	8%	398
Till	9%	57%	15%	10%	10%	293
Sorted sediment	12%	69%	13%	3%	3%	105

3.2 OPLS analysis

The OPLS analysis loading plot showed large variation in performance within and between terrain indices (Fig. 2). Figure 2 only shows the variable names from the best resolution for each digital terrain index and threshold based on the $VIP_{predictive}$

300 value shown in Figure 3, as the graph would be too cluttered if all 146 variable names were displayed. There is an interactive plot in the Supplementary material 2 (S2) where the name of each variable can be found. The general patterns of the effects of scale and threshold are indicated by the size and colour of the dots in the OPLS loading plot (Fig. 2). In order to help the reader to visualize the effects of scales and resolution, the indices and thresholds have been grouped together by using coloured guides to connect terrain indices moving from high to low resolutions.

The OPLS analysis demonstrates that the DTW was a strong predictor of soil moisture classes (Fig. 3), but only if the optimal resolution and stream initiation threshold were used (Fig. 2). DTW loadings were located below zero on the predictive axis due to a negative relationship to soil moisture classes. Generally, the DTW variables were clustered together according to thresholds, with decreasing performance for coarser DEM resolutions. The loading of EAS followed the pattern of DTW and both terrain indices had the highest predictive performance at stream initiation thresholds of 1 and 2 ha in DEM resolutions of 1–4 m. The highest resolutions of 0.5 m had a lower predictive performance (Fig. 2). Increased stream initiation thresholds above 2 ha lowered the predictive performance and added noise, as shown on the orthogonal axis (poso[1]).

The SLU soil moisture and SMI maps both performed well and were the second and fourth best terrain indices, respectively, for predicting soil moisture classes (Fig. 3). SMI scored lower on the predictive axis (pq[1]) and had slightly higher variation not related to the soil moisture classes compared to the SLU soil moisture map (Fig. 2). The SLU soil moisture map and DTW were the best performing soil moisture predictors and had a very similar $VIP_{predictive}$ value (Fig. 3).

Downslope index (DI) was shown to be a good soil moisture class predictor. DI was positively correlated to soil moisture classes and therefore located on the positive pq[1] axis. DI2m (d=2 m) performed better than DI4m (d=4 m) with higher loading on the predictive axis and lower loading on the orthogonal axis. For both DI2m and DI4m, a resolution of 2 m had the highest predictive performance (pq[1]) with the lowest noise. Resolutions below 2 m and above 8 m reduced the performance of the predictions substantially.

The performance of TWI was highly sensitive to the resolution of the DEM, too fine or too coarse resolutions gave nonsensical results. For this landscape, 16 m was found to be the optimal resolution for TWI calculations (Fig. 3). WILT showed the highest value on the positive predictive axis at 8 and 4 m resolution, which was also true for RTP. The WILT loadings were slightly higher than the best performing TWI on the predictive axis (pq[1]), but also much higher on the orthogonal axis, indicating a large variation not related to soil moisture (Fig. 2). RTP showed no clear clustering, similar to TWI, and performed worse compared to the above-mentioned terrain indices (Fig. 3). Plan curvature scored low on the horizontal axis indicating that this variable was not a good soil moisture predictor for this landscape, something also confirmed by the $VIP_{predictive}$ value being below one.
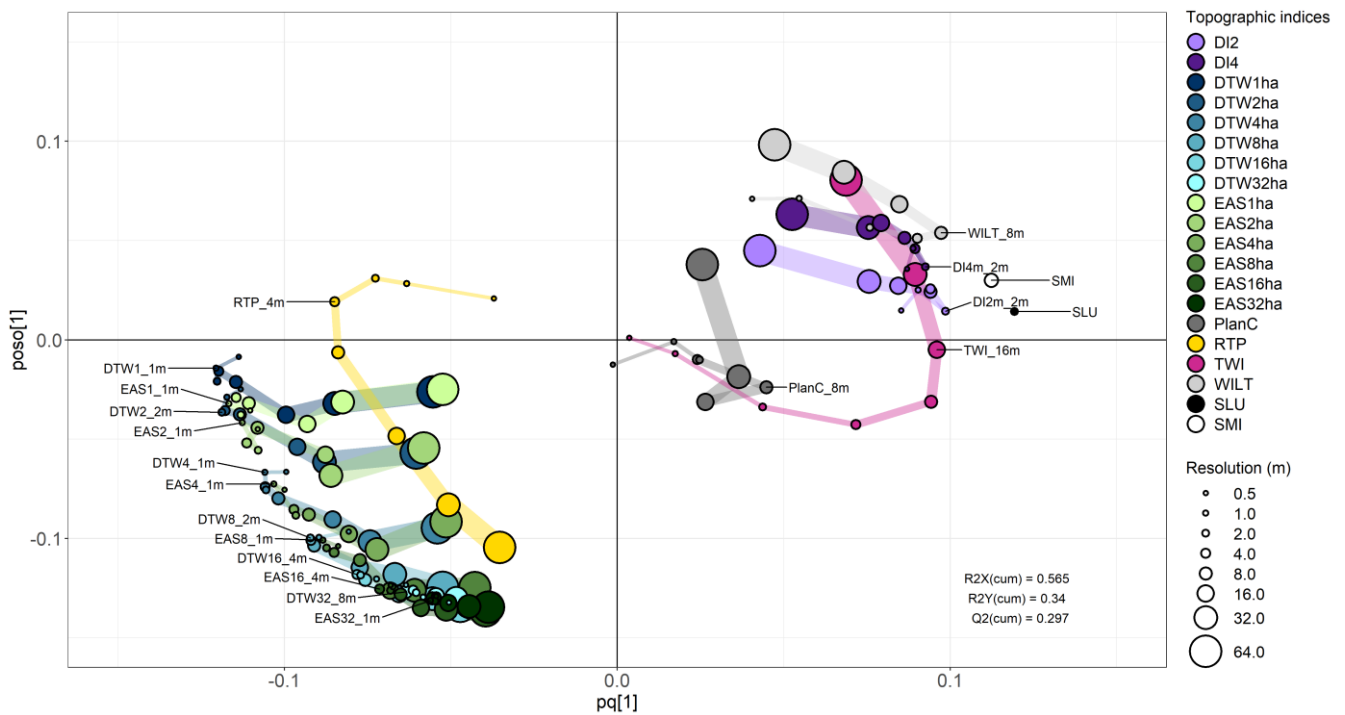
330 **Figure 2. OPLS loading plots for the Krycklan catchment and DEM-derived terrain indices in respect of soil moisture predictions. Variables that cluster closely within the same neighbourhood along the far sides of the horizontal axis are the more robust soil moisture predictors across DEM scales. Coloured guides connect terrain indices moving from small to large resolutions as depicted by the symbol size. In the loading plot, predictive performance increases with increased distance from 0 on the predictive axis (pq[1]). Negative and positive values on the (pq[1]) axis correspond to negative and positive correlations with Y. The orthogonal axis (poso[1])**
335 **represents how much of the variation for each variable was not correlated with the determinant (Y). For the reader who is interested in the details, we have published an electronic version of this graph where all labels are visible by moving the cursor on top of each circle (S2).**
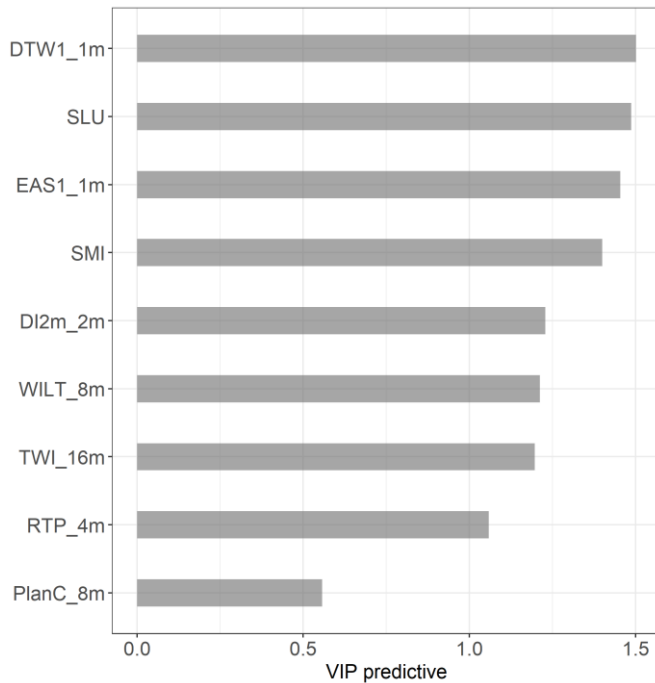
Figure 3. VIP$_{predictive}$ values for the best performing variable for each terrain index. In OPLS, VIP$_{predictive}$ < 1 are variables that are better at explaining Y.

3.3 Visual evaluation

Wet and moist soil conditions within the catchment are mostly found on mires, or as riparian soils along streams as shown in Figure 4. In the IR orthophoto (Fig. 4a), mires can be seen in the flatter areas (Fig. 4b) in the northern parts of the selected area. Several small stream channels in the bottoms of valleys drain the area from northwest to southeast, which borders onto wet riparian soils. Modelled soil moisture conditions of the best performing indices showed similar but varied agreement with natural features when visualized (Fig. 4), with DTW and SLU soil moisture maps clearly delineating the mire in the northwest corner and around the lake, as well as the dryer hilltops in the southeast corner (Fig. 4). With the appropriate resolution and thresholds, many of the terrain indices were able to represent the variation of soil moisture conditions in more or less accurate ways after visual comparison. RTP had a poor performance in the OPLS, which is in line with the results demonstrated in Fig. 4j, where it predicted dry areas within the mire.
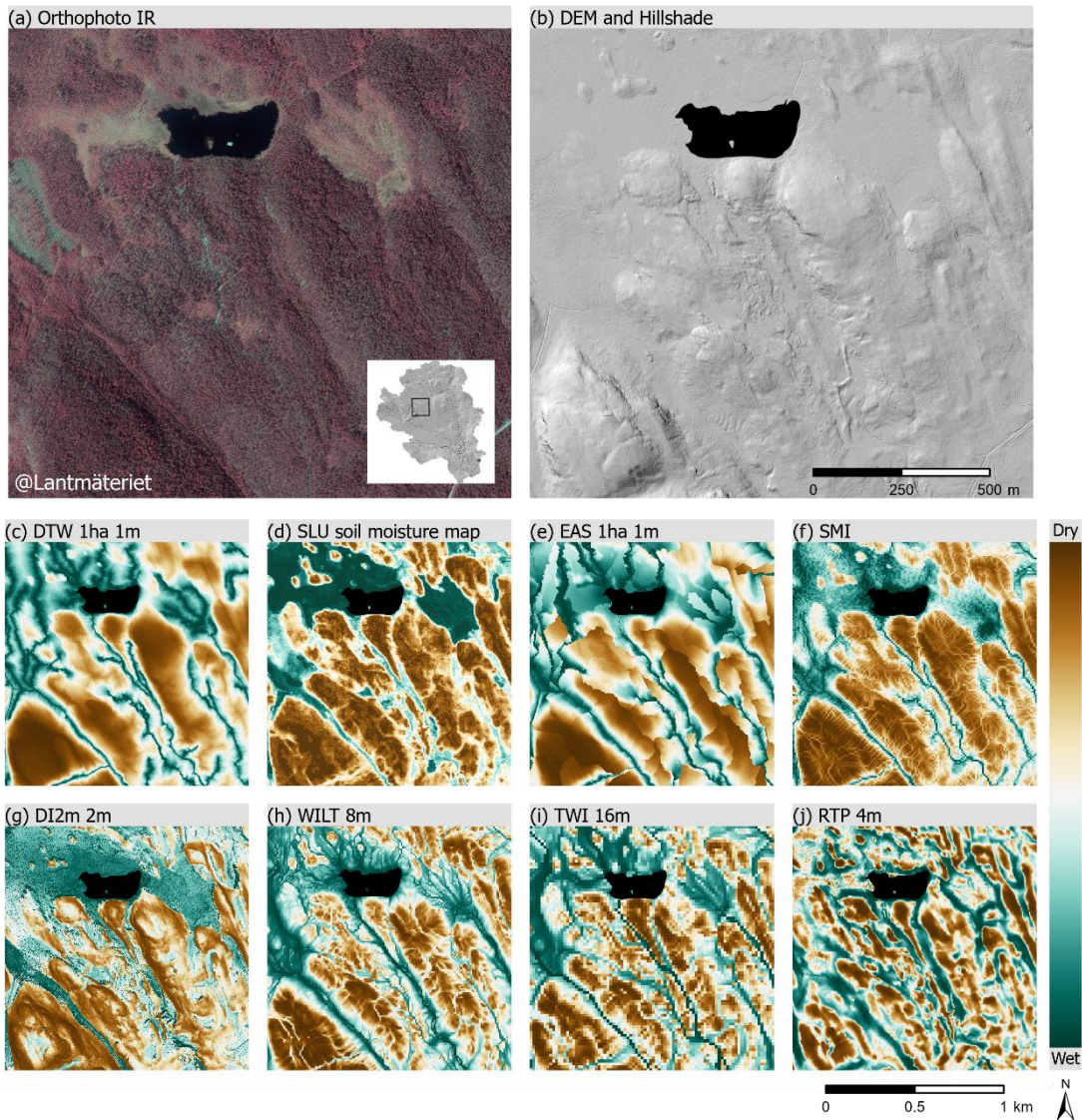
Figure 4. Orthophoto (©Lantmäteriet) (a) and hill-shaded DEM (b) covering a till area within the Krycklan catchment. Below, maps of the highest performing maps of different terrain indices in order of VIP$_{predictive}$ with simplified common symbology for terrain indices (c–j) based on value distribution for the visual comparison.

Figure 5 illustrates differences in the effects of increased DEM resolution represented by modelled results for TWI and DTW with a 1 ha stream flow initiation threshold. Varying DEM resolution had larger effects on the spatial variation of soil moisture conditions using TWI compared to DTW, which was less affected; this is illustrated by the large differences moving from TWI at 1 m resolution to 32 m. The distribution of wet areas was not affected by DEM resolution for DTW compared to TWI. To visualize the effects of different user-defined stream initiation thresholds, DTW maps calculated for 1, 2, 4, 8, 16 and 32 ha

stream networks were created (Fig. 6). Increasing the stream flow initiation threshold shortens the stream network, resulting in a dryer landscape model, and decreasing the stream flow initiation threshold models a wetter landscape.
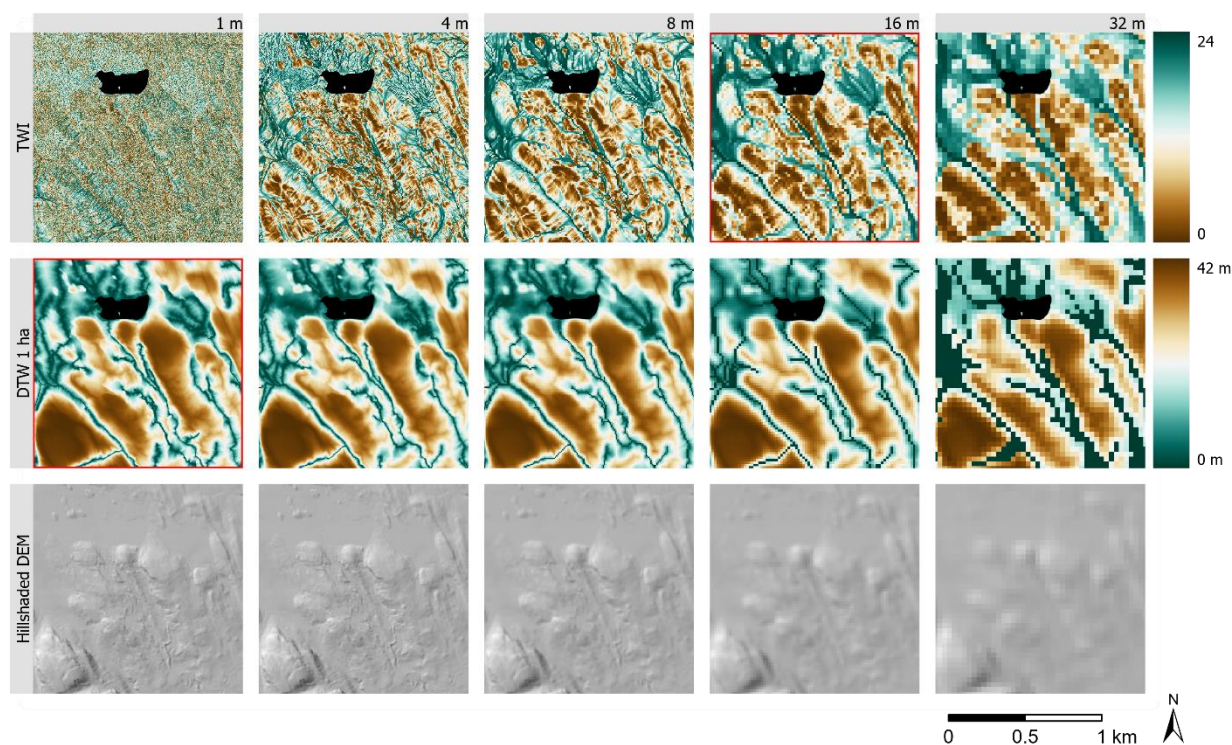
365 **Figure 5. Maps of TWI, DTW and hill-shaded DEM at 1, 4, 8, 16 and 32 m resolution. Best performing rasters in the OPLS analysis are outlined in red.**
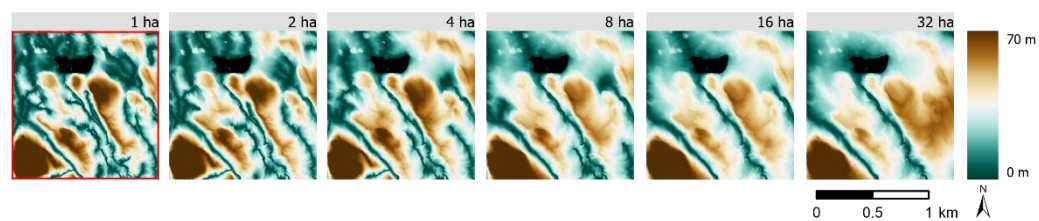
Figure 6. Maps of DTW at 1 m resolution with stream initiation thresholds from 1 to 32 ha.

3.4 Confusion matrix

The overall agreement of DTW 1m 1ha values (DTW<1) in relation to wet and moist soil classes was further tested using a confusion matrix (Table 3). Over the entire catchment area, the accuracy was 77% with a MCC of 0.42. Dividing the catchment into till and sorted sediment areas revealed significant differences in conformance. On the till area of the catchment, the DTW accuracy was higher with an accuracy of 78% and a MCC of 0.50. On the sorted sediment area of the catchment, DTW falsely predicted a large proportion of the dry plots as wet (FP). Only a third of the wet plots were predicted as wet (TP). The overall accuracy was better for the SLU soil moisture map however showed the same pattern as DTW in the sorted sediment area with a low MCC value of 0.34%.

Table 3. Confusion matrix of true positives (TP), true negatives (TN), false positives (FP) and false negatives (FN), representing Wet (Positive) and Dry (Negative) plots predicted by DTW 1 ha at 1 m resolution and the SLU soil moisture map, as well as prediction accuracy (ACC (%)) and Matthews Correlation Coefficient (MCC (%)). Confusion matrixes and statistics were calculated for the entire catchment and divided into till and sorted sediment areas.

	Area	Plots (n)	TP	TN	FP	FN	ACC (%)	MCC
DTW	Entire catchment	398	61	245	61	31	77	0.42
	Till	293	53	176	49	15	78	0.50
	Sorted sediment	105	8	69	12	16	73	0.20
SLU	Entire catchment	398	78	255	21	44	84	0.60
	Till	293	69	180	11	33	85	0.66
	Sorted sediment	105	9	75	10	11	80	0.34

4 Discussion

Modelling the spatial patterns of soil moisture remains an important scientific challenge and terrain indices are potentially a useful tool. As the availability and resolution of DEMs have increased, so have the uses of terrain indices for modelling hydrological, environmental and soil properties. However, the predictive performance of terrain indices is highly dependent on identifying the optimal spatial scales and user-defined thresholds for modelling soil moisture (Sørensen and Seibert, 2007; Lin et al., 2010; Ågren et al., 2014). The aim of this study, was therefore, to evaluate how DEM resolution, user-defined thresholds and landscape types affect soil moisture predictions from a range of readily available terrain indices in relation to

field-classified soil moisture conditions across a boreal catchment. Our results demonstrate the potential of terrain indices for modelling soil moisture when the optimal DEM resolutions and user-defined thresholds are selected. No previous study has been able to provide such detailed data at catchment scale, amount of terrain indices in combination with an extensive field survey which clearly demonstrates the importance of selection of terrain index, DEM resolution and index-specific thresholds.

395   Several terrain indices were able to predict the spatial variation of soil moisture classes within our study area, however our results revealed a large variation in the predictive performance within, and between, terrain indices at different DEM resolutions and index-specific thresholds (Fig. 3). The general agreement of appropriately scaled terrain indices with field classified soil moisture conditions (Fig. 2) and visualized maps (Fig. 4) supports the underlying assumption that topography acts as the main driver of spatially varying soil moisture conditions. This is in line with many previous studies relating terrain

400   indices to soil moisture conditions (Lin et al., 2010; Seibert et al., 2007; Grabs et al., 2009; Murphy et al., 2011; Ågren et al., 2014) and groundwater levels (Rinderer et al., 2014).

        Ground truthing is required to evaluate the performance of different terrain indices, to prevent inappropriate choices of resolution and user-defined thresholds resulting in non-representative predictions of soil moisture. As its ground truth, this study used a uniquely extensive and high precision field survey within a well-studied landscape. We used field-mapped soil

405   moisture classes based on estimated depth to groundwater from the soil surface guided by surrounding topography and vegetation patterns as a proxy for average soil moisture conditions, thus reducing the uncertainty associated with the large temporal and small-scale spatial variability of soil moisture (Murphy et al., 2011; Oltean et al., 2016; Beucher et al., 2019; Lidberg et al., 2019). The position in the landscape and the vegetation patterns that form the basis for the classifications stay constant over time. In contrast, more direct soil moisture measurements using values such as soil water content and Time

410   Domain Reflectometry (TDR) are greatly affected by the specific weather conditions before, and at the moment of, measurement. On the other hand, by using soil moisture classes as the ground truth, we only evaluate the "average" soil moisture conditions for each site and thereby focus on the spatial variability of relative soil moisture conditions within the landscape. We do, however, acknowledge that soil moisture varies greatly with season and depends on regional weather conditions causing stream networks and wet soils to expand and shrink during the year (Ågren et al., 2015).

415   Our results highlight that the optimum DEM resolution for soil moisture predictions differed depending on terrain index, and further demonstrated the large effects of DEM resolution within certain terrain indices (Fig. 5). In line with previous studies, TWI was greatly affected by DEM resolution and was shown to perform best with a coarser 16 m resolution while performing poorly with high resolution DEMs. This agrees well with previous studies both within (Sørensen and Seibert, 2007; Ågren et al., 2014) and outside the study area (Lin et al., 2010; Murphy et al., 2011). However, this is in contrast to a recent

420   study by (Riihimäki et al., 2021) where they thoroughly investigated the effect of DEM resolution and flow accumulation algorithms on TWI calculations in a 300 ha area of the northwestern Fennoscandian mountain tundra. Their conclusion was that Dinf reached its maximum explanatory power at 3 m resolution. This highlights that the optimal DEM resolution for predicting soil moisture conditions using TWI cannot just be taken from literature as it varies from site to site and it's necessary to investigate the optimal resolution for each landscape. While this has previously been shown in the literature, a concern with

425   the rapidly increasing numbers of high resolution DEMs worldwide is that researchers will use the most commonly used terrain index TWI, and disregard its poor performance with high resolution DEMs. Other indices, such as DTW, EAS and DI, had the best performance for resolutions between 1 and 4 m, and were stable within this range, as shown for DTW in Figure 5. When using high resolution DEMs, the importance of selecting the optimal method for the pre-processing step (the hydrological corrections of depressions) increases. The impoundments caused by road banks (that are captured in high-resolution DEMs)

430   otherwise cause problems for the subsequent steps of modelling the flow paths in the landscape (Woodrow et al., 2016; Leach et al., 2017). Studies have shown that it is better to pre-process the DEM using breaching, rather than filling functions (Wang et al., 2019; Lidberg et al., 2017). In this study, we used the protocol suggested by Lidberg et al. (2017), as that study was carried out on similar glaciated catchments in Sweden. The highest resolution of DEM did not perform optimally for any of the evaluated terrain indices. This has been highlighted by previous studies to be caused by small-scale variations in surface

435   topography that do not affect the overall hydrological pathways (Gillin et al., 2015). The dependency of DEM resolution is important for any type of digital soil mapping and the optimum resolutions have been shown to be different, depending on landscape and the spatial scale of the environmental phenomena and processes involved in the soil property of interest (Cavazzi et al., 2013).

        This study also demonstrated the effects of adjusting user-defined thresholds associated with certain indices

440   calculations (Fig. 2 & Fig. 6). In line with a previous study modelling the spatial extent of wet areas, DI calculated with a 2 m given vertical distance (d) (Eq. 3) performed best (Hjerdt et al., 2004). DTW and EAS were among the best performing terrain indices (Fig. 3), however the overall predictive performance was dependent on the chosen stream initiation thresholds (Fig. 2). The best performance was achieved at 1 ha followed by 2 ha stream flow initiation threshold, much in line with previous results from the studied catchment area (Ågren et al., 2014), and from other study areas (Oltean et al., 2016). However, that only

445   means that those thresholds might work well for glaciated catchments: in other regions, these thresholds might need to be adjusted. Again, our study highlights the need for ground truthing of the digital terrain indices, as the quality of the generated maps are so dependent on the selected thresholds. The substantial effects of varied user-defined thresholds for DTW and EAS highlights the importance of caution when selecting terrain indices.

        The unique setting of the Krycklan catchment, with its heterogeneous soils, made it possible for this study to

450   demonstrate the challenges raised from variable landform types, where the assumption of topography acting as a first order control of soil moisture becomes less valid. In the sorted sediment areas of the Krycklan catchment, topographic variation is low and hydraulic conductivity high, allowing for deeper infiltration of water which decreases the topographical control of groundwater flows compared to the upper till which dominates parts of the catchment (Jutebring Sterte et al., 2021). The layout of the study did not allow separate analysis of the different land form classes due to the limited number of field plots and low

455   variation of soil moisture classes in the sorted sediment area (Table 1). However, by using a confusion matrix of the classified best performing terrain index (DTW < 1 m) from the OPLS in conformance with wet and dry soils, this study demonstrated a large difference in the MCC values between the sorted sediment (0.20) and till (0.50) parts of the catchment. The attempts of combining terrain indices and other mapped information to tackle the challenges of soil moisture modelling faced by landscape

heterogeneity did not outperform the more basic terrain indices at the entire catchment level. The confusion matrix using the
SLU map and DTW's overall conformance clearly showed the challenges caused by the sorted sediment areas of the catchment
(Table 3). This study highlights the necessity of adapting soil moisture predictions to local soil conditions. These underlying
factors need to be taken into consideration when modelling soil moisture conditions on any level from catchment, regional and
national scale. One such attempt was the SLU soil moisture map which was constructed for the entire country of Sweden using
vast amounts of field data from 16 000 field-plots across the country as training data and several digital terrain indices at
multiple resolutions and thresholds. Even so, when evaluated on the Krycklan catchment the SLU soil moisture map ranked
second among the top predictors for soil moisture (Figure 2 and 3) and did not outperform several of the more simple terrain
indices.

The results from this study demonstrate the potential of terrain indices for modelling soil moisture across the
landscape when the optimal scales and thresholds are selected for the calculations. Terrain indices have been related to soil
properties (Seibert et al., 2007; Zajícová and Chuman, 2021), ecological studies (Zinko et al., 2005; Bartels et al., 2018) and
site productivity (Mohamedou et al., 2017; Bjelanovic et al., 2018), and will likely develop further as a useful tool within many
fields of study. However, it should be recognized that the predictive power of terrain indices is limited by the non-topographical
drivers of the spatial variation in soil moisture which will always be significant, and rarely less than 50% (Western et al.,
1999). Such drivers are, for example, soil depth, texture, hydrological conductivity, permeability and vegetation (Gwak and
Kim, 2017). With an increasing demand for high-resolution spatial and temporal soil moisture models for climate, hydrology
and soil modelling, it is important to understand underlying the covariate factors used to build them.

5 Conclusion

This study was designed to test, demonstrate and visualize the importance of appropriate scaling when modelling soil moisture
conditions using terrain indices. Although some previous studies have drawn similar conclusions, there is still a tendency
within many fields to use the highest DEM resolution available when using terrain indices to represent soil moisture conditions
as a covariate. However, one size - or resolution in this case - does not fit all. Due to the differences in climate, landscape types
and soil texture, terrain indices must be adapted to local conditions and calculated at appropriate scales and thresholds.
Heterogeneous landscape types remain a challenge for predicting soil moisture conditions and should be taken into account
when interpreting modelled results. We, therefore, stress the importance of evaluating the modelled terrain index results for
the area of interest and not to extrapolate the optimum terrain indices for our study areas directly or to blindly use the DEM of
highest resolution available.

6 Code and data availability

The code and data used in this study for aggregating the DEM and generating the different terrain indices is available
490 **in Supplementary material 1 (S1). 7 Supplement**

The supplementary material related to this article S1 and S2 is available online at:

https://data.mendeley.com/datasets/dg64p8wmj9/draft?a=3ca61bcf-627a-4a26-93ea-5b4327a8eaab

495 ## 8 Author contribution

All authors were responsible for the conceptualization of the study and evaluation of results. WL was responsible for the data curation and JL performed the analysis. JL prepared the manuscript and figures and lead the writing of the paper with contributions from all the co-authors.

9 Competing interests

500 The authors declare that they have no conflict of interest.

References

Abowarda, A. S., Bai, L., Zhang, C., Long, D., Li, X., Huang, Q., and Sun, Z.: Generating surface soil moisture at 30 m spatial resolution using both data fusion and machine learning toward better water resources management at the field scale, Remote Sensing of Environment, 255, 112301, https://doi.org/10.1016/j.rse.2021.112301, 2021.

505 Ågren, A., Lidberg, W., Strömgren, M., Ogilvie, J., and Arp, P.: Evaluating digital terrain indices for soil wetness mapping – A Swedish case study, Hydrology and Earth System Sciences Discussions, 11, https://doi.org/10.5194/hessd-11-4103-2014, 2014.

Ågren, A. M., Lidberg, W., and Ring, E.: Mapping Temporal Dynamics in a Forest Stream Network—Implications for Riparian Forest Management, 6, 2982–3001, https://doi.org/10.3390/f6092982, 2015.

510 Ågren, A. M., Larson, J., Paul, S. S., Laudon, H., and Lidberg, W.: Use of multiple LIDAR-derived digital terrain indices and machine learning for high-resolution national-scale soil moisture mapping of the Swedish forest landscape, Geoderma, 404, 115280, https://doi.org/10.1016/j.geoderma.2021.115280, 2021.

Bachmair, S. and Weiler, M.: New Dimensions of Hillslope Hydrology, in: Forest Hydrology and Biogeochemistry: Synthesis of Past Research and Future Directions, edited by: Levia, D. F., Carlyle-Moses, D., and Tanaka, T., Springer Netherlands, 515 Dordrecht, 455–481, https://doi.org/10.1007/978-94-007-1363-5_23, 2011.

Bartels, S., Caners, R., Ogilvie, J., White, B., and Macdonald, S.: Relating Bryophyte Assemblages to a Remotely Sensed Depth-to-Water Index in Boreal Forests, https://doi.org/10.3389/fpls.2018.00858, 2018.

Beucher, A., Møller, A. B., and Greve, M. H.: Artificial neural networks and decision tree classification for predicting soil drainage classes in Denmark, Geoderma, 352, 351–359, https://doi.org/10.1016/j.geoderma.2017.11.004, 2019.

520 Beven, K. J. and Kirkby, M. J.: A physically based, variable contributing area model of basin hydrology / Un modèle à base physique de zone d'appel variable de l'hydrologie du bassin versant, 24, 43–69, https://doi.org/10.1080/02626667909491834, 1979.

Bjelanovic, I., Comeau, P., and White, B.: High Resolution Site Index Prediction in Boreal Forests Using Topographic and Wet Areas Mapping Attributes, 9, 113, 2018.

525 Boughorbel, S., Jarray, F., and El-Anbari, M.: Optimal classifier for imbalanced data using Matthews Correlation Coefficient metric, PLOS ONE, 12, e0177678, https://doi.org/10.1371/journal.pone.0177678, 2017.

Buchanan, B., Fleming, M. L., Schneider, R., Richards, B., Archibald, J., Qiu, Z., and Walter, M.: Evaluating topographic wetness indices across Central New York agricultural landscapes, Hydrology and Earth System Sciences Discussions, 10, 14041–14093, https://doi.org/10.5194/hessd-10-14041-2013, 2013.

530 Cavazzi, S., Corstanje, R., Mayr, T., Hannam, J., and Fealy, R.: Are fine resolution digital elevation models always the best choice in digital soil mapping?, Geoderma, 195–196, 111–121, https://doi.org/10.1016/j.geoderma.2012.11.020, 2013.

Eriksson, L., Johansson, E., Kettaneh-Wold, N., Trygg, J., Wikstr, C., and Wold, S.: Multi- and Megavariate Data Analysis. Part I Basic Principles and Applications. Second revised and enlarged edition, Ume Sweden: MKS Umetrics AB, 1–103, 2006.

Florinsky, I. V.: Chapter 9 - Influence of Topography on Soil Properties, in: Digital Terrain Analysis in Soil Science and 535 Geology (Second Edition), edited by: Florinsky, I. V., Academic Press, 265–270, https://doi.org/10.1016/B978-0-12-804632-6.00009-2, 2016.

Fridman, J., Holm, S., Nilsson, M., Nilsson, P., Hedstrom Ringvall, A., and Ståhl, G.: Adapting National Forest Inventories to changing requirements - The case of the Swedish National Forest Inventory at the turn of the 20th century, 48, https://doi.org/10.14214/sf.1095, 2014.

540 Gillin, C., Bailey, S., McGuire, K., and Prisley, S.: Evaluation of Lidar-derived DEMs through Terrain Analysis and Field Comparison, Photogrammetric Engineering & Remote Sensing, 81, 387–396, https://doi.org/10.14358/PERS.81.5.387, 2015.

Grabs, T., Seibert, J., Bishop, K., and Laudon, H.: Modeling spatial patterns of saturated areas: A comparison of the topographic wetness index and a dynamic distributed model, Journal of Hydrology, 373, 15–23, https://doi.org/10.1016/j.jhydrol.2009.03.031, 2009.

545 Güntner, A., Seibert, J., and Uhlenbrook, S.: Modeling spatial patterns of saturated areas: An evaluation of different terrain indices, Water Resources Research, 40, https://doi.org/10.1029/2003WR002864, 2004.

Gwak, Y. and Kim, S.: Factors affecting soil moisture spatial variability for a humid forest hillslope, Hydrological Processes, 31, 431–445, https://doi.org/10.1002/hyp.11039, 2017.

Hjerdt, K. N., McDonnell, J. J., Seibert, J., and Rodhe, A.: A new topographic index to quantify downslope controls on local 550 drainage, Water Resources Research, 40, https://doi.org/10.1029/2004WR003130, 2004.

Högberg, P., Näsholm, T., Franklin, O., and Högberg, M.: Tamm Review: On the nature of the nitrogen limitation to plant growth in Fennoscandian boreal forests, https://doi.org/10.1016/j.foreco.2017.04.045, 2017.

Jutebring Sterte, E., Lidman, F., Lindborg, E., Sjöberg, Y., and Laudon, H.: How catchment characteristics influence hydrological pathways and travel times in a boreal landscape, 25, 2133–2158, https://doi.org/10.5194/hess-25-2133-2021, 555 2021.

Kopecký, M., Macek, M., and Wild, J.: Topographic Wetness Index calculation guidelines based on measured soil moisture and plant species composition, Science of The Total Environment, 757, 143785, https://doi.org/10.1016/j.scitotenv.2020.143785, 2021.

Koster, R. D., Mahanama, S. P. P., Livneh, B., Lettenmaier, D. P., and Reichle, R. H.: Skill in streamflow forecasts derived 560 from large-scale estimates of soil moisture and snow, Nature Geoscience, 3, 613–616, https://doi.org/10.1038/ngeo944, 2010.

Laudon, H., Taberman, I., Ågren, A., Futter, M., Ottosson-Löfvenius, M., and Bishop, K.: The Krycklan Catchment Study— A flagship infrastructure for hydrology, biogeochemistry, and climate research in the boreal landscape, 49, 7154–7158, https://doi.org/10.1002/wrcr.20520, 2013.

Laudon, H., Hasselquist, E. M., Peichl, M., Lindgren, K., Sponseller, R., Lidman, F., Kuglerova, L., Hasselquist, N., Bishop, 565 K., and Nilsson, M.: Northern landscapes in transition; evidence, approach and ways forward using the Krycklan Catchment Study, Authorea Preprints, 2020.

Leach, J. A., Lidberg, W., Kuglerová, L., Peralta-Tapia, A., Ågren, A., and Laudon, H.: Evaluating topography-based predictions of shallow lateral groundwater discharge zones for a boreal lake-stream system, Water Resources Research, 53, 5420–5437, https://doi.org/10.1002/2016WR019804, 2017.

570 Lidberg, W., Nilsson, M., Lundmark, T., and Ågren, A. M.: Evaluating preprocessing methods of digital elevation models for hydrological modelling, 31, 4660–4668, https://doi.org/10.1002/hyp.11385, 2017.

Lidberg, W., Nilsson, M., and Ågren, A.: Using machine learning to generate high-resolution wet area maps for planning forest management: A study in a boreal forest landscape, AMBIO A Journal of the Human Environment, https://doi.org/10.1007/s13280-019-01196-9, 2019.

575 Lin, K., Zhang, Q., and Chen, X.: An evaluation of impacts of DEM resolution and parameter correlation on TOPMODEL modeling uncertainty, Journal of Hydrology, 394, 370–383, https://doi.org/10.1016/j.jhydrol.2010.09.012, 2010.

Lindsay, J. B.: Efficient hybrid breaching-filling sink removal methods for flow path enforcement in digital elevation models, Hydrological Processes, 30, 846–857, https://doi.org/10.1002/hyp.10648, 2016a.

Lindsay, J. B.: Whitebox GAT: A case study in geomorphometric analysis, Computers & Geosciences, 95, 75–84,
580 https://doi.org/10.1016/j.cageo.2016.07.003, 2016b.

Meles, M. B., Younger, S. E., Jackson, C. R., Du, E., and Drover, D.: Wetness index based on landscape position and topography (WILT): Modifying TWI to reflect landscape position, Journal of Environmental Management, 255, 109863, https://doi.org/10.1016/j.jenvman.2019.109863, 2020.

Mohamedou, C., Tokola, T., and Eerikäinen, K.: LiDAR-based TWI and terrain attributes in improving parametric predictor
585 for tree growth in southeast Finland, International Journal of Applied Earth Observation and Geoinformation, 62, 183–191, https://doi.org/10.1016/j.jag.2017.06.004, 2017.

Murphy, P. N. C., Ogilvie, J., Castonguay, M., Zhang, C., Meng, F.-R., and Arp, P. A.: Improving forest operations planning through high-resolution flow-channel and wet-areas mapping, The Forestry Chronicle, 84, 568–574, https://doi.org/10.5558/tfc84568-4, 2008.

590 Murphy, P. N. C., Ogilvie, J., Meng, F.-R., White, B., Bhatti, J. S., and Arp, P. A.: Modelling and mapping topographic variations in forest soils at high resolution: A case study, 222, 2314–2332, https://doi.org/10.1016/j.ecolmodel.2011.01.003, 2011.

Naturvårdsverket: The National Land Cover Database: Soil moisture index map, 2021.

O, S., Hou, X., and Orth, R.: Observational evidence of wildfire-promoting soil moisture anomalies, Scientific Reports, 10,
595 11008, https://doi.org/10.1038/s41598-020-67530-4, 2020.

O'Callaghan, J. F. and Mark, D. M.: The extraction of drainage networks from digital elevation data, Computer Vision, Graphics, and Image Processing, 28, 323–344, https://doi.org/10.1016/S0734-189X(84)80011-0, 1984.

Olsson, M. T., Erlandsson, M., Lundin, L., Nilsson, T., Nilsson, Å., and Stendahl, J.: Organic carbon stocks in Swedish Podzol soils in relation to soil hydrology and other site characteristics, 43, 209–222, 2009.

600 Oltean, G. S., Comeau, P., and White, B.: Linking the Depth-to-Water Topographic Index to Soil Moisture on Boreal Forest Sites in Alberta, 154 pp., https://doi.org/10.5849/forsci.15-054, 2016.

Quinn, P. F., Beven, K. J., and Lamb, R.: The in(a/tan/β) index: How to calculate it and how to use it within the topmodel framework, Hydrological Processes, 9, 161–182, https://doi.org/10.1002/hyp.3360090204, 1995.

R Core Team: R: A Language and Environment for Statistical Computing, R Foundation for Statistical Computing, Vienna,
605 Austria, 2020.

Rennó, C. D., Nobre, A. D., Cuartas, L. A., Soares, J. V., Hodnett, M. G., Tomasella, J., and Waterloo, M. J.: HAND, a new terrain descriptor using SRTM-DEM: Mapping terra-firme rainforest environments in Amazonia, Remote Sensing of Environment, 112, 3469–3481, https://doi.org/10.1016/j.rse.2008.03.018, 2008.

Riihimäki, H., Kemppinen, J., Kopecký, M., and Luoto, M.: Topographic Wetness Index as a Proxy for Soil Moisture: The Importance of Flow-Routing Algorithm and Grid Resolution, Water Resources Research, 57, e2021WR029871, https://doi.org/10.1029/2021WR029871, 2021.

Rinderer, M., van Meerveld, H. J., and Seibert, J.: Topographic controls on shallow groundwater levels in a steep, prealpine catchment: When are the TWI assumptions valid?, Water Resources Research, 50, 6067–6080, https://doi.org/10.1002/2013WR015009, 2014.

Robock, A.: HYDROLOGY, FLOODS AND DROUGHTS | Soil Moisture, in: Encyclopedia of Atmospheric Sciences (Second Edition), edited by: North, G. R., Pyle, J., and Zhang, F., Academic Press, Oxford, 232–239, https://doi.org/10.1016/B978-0-12-382225-3.00169-9, 2015.

Rodhe, A.: The origin of streamwater traced by oxygen-18, Doctoral thesis, monograph, Uppsala University, Knivsta, 260 pp., 1987.

Seibert, J. and McGlynn, B. L.: A new triangular multiple flow direction algorithm for computing upslope areas from gridded digital elevation models, 43, https://doi.org/10.1029/2006WR005128, 2007.

Seibert, J., Stendahl, J., and Sørensen, R.: Topographical Influences on Soil Properties in Boreal Forests, Geoderma, 141, 139–148, https://doi.org/10.1016/j.geoderma.2007.05.013, 2007.

Sørensen, R. and Seibert, J.: Effects of DEM resolution on the calculation of topographical indices: TWI and its components, Journal of Hydrology, 347, 79–89, https://doi.org/10.1016/j.jhydrol.2007.09.001, 2007.

Sørensen, R., Zinko, U., and Seibert, J.: On the calculation of the topographic wetness index: evaluation of different methods based on field observations, 10, 101–112, 2006.

Swedish NFI: Fältinstruktion 2014 RIS-Riksinventeringen av skog, Swedish University of Agricultural Sciences, Department of Forest Resource management, 2014.

Tarboton, D. G.: A new method for the determination of flow directions and upslope areas in grid digital elevation models, Water Resources Research, 33, 309–319, https://doi.org/10.1029/96WR03137, 1997.

Wang, C., Fu, B., Zhang, L., and Xu, Z.: Soil moisture–plant interactions: an ecohydrological review, Journal of Soils and Sediments, 19, 1–9, https://doi.org/10.1007/s11368-018-2167-0, 2019.

Western, A. W., Grayson, R. B., Blöschl, G., Willgoose, G. R., and McMahon, T. A.: Observed spatial organization of soil moisture and its relation to terrain indices, Water Resources Research, 35, 797–810, https://doi.org/10.1029/1998WR900065, 1999.

Wickham, H.: ggplot2: Elegant Graphics for Data Analysis, Springer-Verlag, New York, 2016.

Wilson, J. P. and Gallant, J. C.: Terrain analysis: principles and applications, John Wiley & Sons, 2000.

Woodrow, K., Lindsay, J. B., and Berg, A. A.: Evaluating DEM conditioning techniques, elevation source data, and grid
640   resolution for field-scale hydrological parameter extraction, Journal of Hydrology, 540, 1022–1029, https://doi.org/10.1016/j.jhydrol.2016.07.018, 2016.

Zajícová, K. and Chuman, T.: Spatial variability of forest floor and topsoil thicknesses and their relation to topography and forest stand characteristics in managed forests of Norway spruce and European beech, European Journal of Forest Research, 140, 77–90, https://doi.org/10.1007/s10342-020-01316-1, 2021.

645   Zhu, Q. and Lin, H.: Influences of soil, terrain, and crop growth on soil moisture variation from transect to farm scales, Geoderma, 163, 45–54, https://doi.org/10.1016/j.geoderma.2011.03.015, 2011.

Zinko, U., Seibert, J., Dynesius, M., and Nilsson, C.: Plant Species Numbers Predicted by a Topography-based Groundwater Flow Index, 8, 430–441, https://doi.org/10.1007/pl00021513, 2005.